INVESTIGATIONS INTO THE FAILURE OF CONCRETE RINGS UNDER INNER PRESSURE

G.A. Plizzari,
University of Brescia, Dept. of Civil Engineering, Italy
T. Klink and V. Slowik,
Hochschule für Technik, Wirtschaft und Kultur Leipzig (FH), Germany

Abstract
Thick-walled concrete rings were subjected to an inner pressure to simulate the wedge forces provoked by the ribs of reinforcing bars in concrete. In order to realistically represent the actual wedge action resulting from the pull-out of a ribbed bar, a special mechanical loading device has been used to apply an outward displacement to the inner surface of the ring. The influence of the external confinement on the damage localization and on the splitting crack development was studied in the experiments. Numerical analyses were performed by utilizing a discrete as well as a smeared crack approach.
Key words: Steel-Concrete Bond, Splitting Cracks, Reinforced Concrete

1 Introduction

In anchorages and overlapping splices with highly stressed ribbed bars, splitting cracks may occur in the concrete cover because of the wedge action of the ribs. As far as bond failure is concerned, concrete splitting is still a topical problem. New approaches are being provided by concrete fracture mechanics, which may lead to a better understanding of the local bond behavior of a rebar.

With reference to local resistance mechanisms, some limit analysis models have been developed to describe the formation of the splitting cracks and the hoop action in a concrete ring subjected to an outward pressure simulating the wedge action of the ribs (Tepfers, 1979; Reinhardt and van der Veen, 1990; Balaguru et al., 1995; Noghabai, 1995). These models predict the maximum pressure applicable to the inner ring and some of them include crack cohesion along the splitting cracks. A crucial aspect of the problem is represented by the exact number of splitting cracks that form in the concrete ring surrounding the reinforcing bar (Balaguru et al., 1995).

The aim of this work is to experimentally investigate the fracture process in thick-walled concrete rings. In order to simulate the wedge action of the ribs of an actual rebar, the specimens were loaded by imposing an outward deformation to the inner ring. Specimens with different external confinements were adopted to simulate the effects of large concrete covers, transverse reinforcement or external pressure. Furthermore, the rib shape of the deformed bars often used in practice is not circular so that a non-uniform wedge action is applied to the concrete. In order to shed some new light on these aspects that may influence the splitting crack pattern, numerical FE analyses were performed by using both a discrete and a smeared crack approach. The results intend to contribute to a better understanding of the splitting crack development in the concrete surrounding a deformed bar.

2 Experiments

2.1 Specimens and loading device

The specimen geometry is shown in Fig. 1. All six samples had a thickness of 60 mm, an inner diameter of 82.1 mm and an outer diameter of 500 mm. Electric strain gages having a length of 40 mm were used to monitor the deformations during the experiments (Fig. 1).

To impose an outward radial displacement to the inner circumference, a mechanical loading device was used (Fig. 2). By turning a threaded center bolt, conic metal pieces were moved in axial direction from the inside of the loading device pressing the 12 metal beams in the radial direction. To minimize radial stress concentrations, 12 thin steel segments were placed between the beams and the concrete surface.

As a rebar in concrete, the loading device imposes a uniform displacement to the concrete surface. In order to provide a uniform contact between the loading device and the concrete ring, a precisely manufactured circular cylinder made of plastics was used as an inner form piece. Before starting the test, this piece was replaced by the loading device.
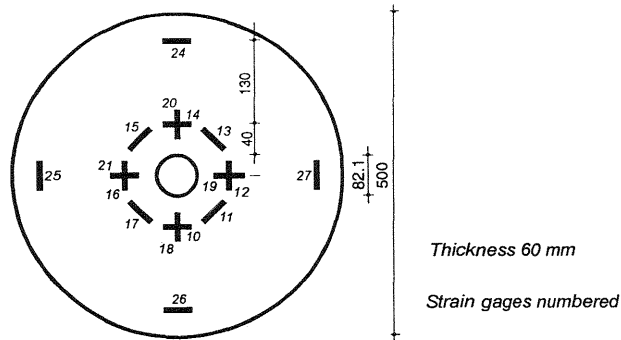
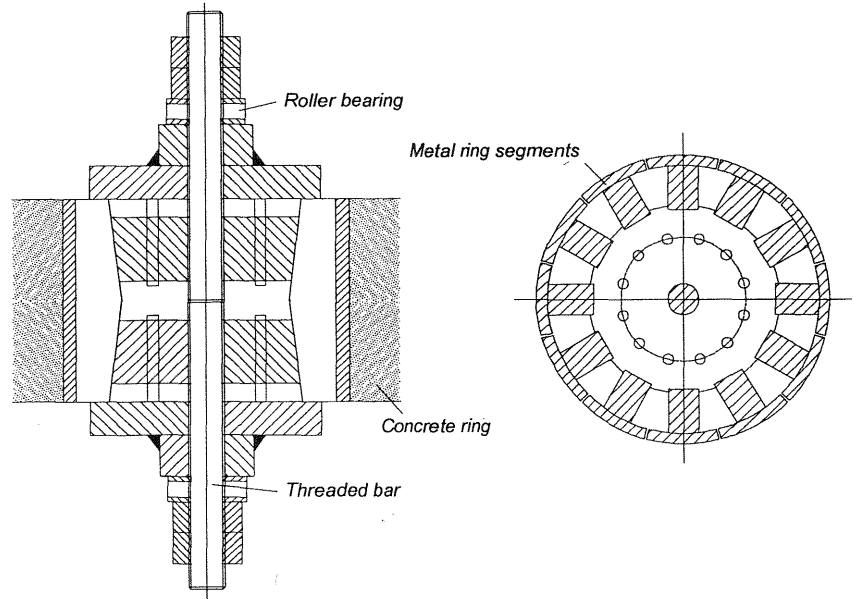Fig. 1. Specimen geometry and strain gage arrangement

Fig. 2. Loading device

In most of the experiments, a 3 mm thick metal ring was placed around the outer surface of the thick-walled concrete ring. The metal ring consisted of three segments. The joints between the ring segments could be tightened to impose a certain pre-strain to the specimen which was measured by strain gages applied to the metal ring. The prestrain values for the samples are shown in Fig. 3. At the interface between the concrete and the steel ring, grease was applied in order to reduce friction stresses.

2.2 Material properties
Concrete with a compressive strength of about 45 MPa and an elasticity modulus of about 26000 MPa was used. The maximum aggregate size

amounted to 8 mm. After casting, the samples were stored under water and tested at an age varying between 24 and 34 days.

The concrete fracture properties were determined from six wedge splitting tests (specimen height=300 mm, ligament length=165 mm). The average specific fracture energy amounted to about 100 N/m. The softening behavior was determined by a backward Finite-Element analysis assuming a bilinear softening curve. The best fitting coefficients are the following: tensile strength f_{ct}=3.6 MPa, break point coordinates w_l=0.02 mm and σ_l=0.63 MPa, critical crack opening w_c=0.2 mm.

2.3 Experimental observations

The final crack patterns for the six samples are exhibited in Fig. 3.

In the specimen without external ring (Ring 1), two radial cracks formed on opposite sides of the ring (Noghabai, 1995). One of them (called primary crack), stretched from the inside to the outside of the concrete ring. The other one (secondary crack), started from the inside and ended within the concrete ring. The crack propagation became unstable soon after the elastic limit strain was reached at the gage locations, which means that only a short fracture process zone could develop in a stable manner.

In specimens having the external steel ring (confined specimens), a different crack pattern was observed; in fact, three or four cracks formed
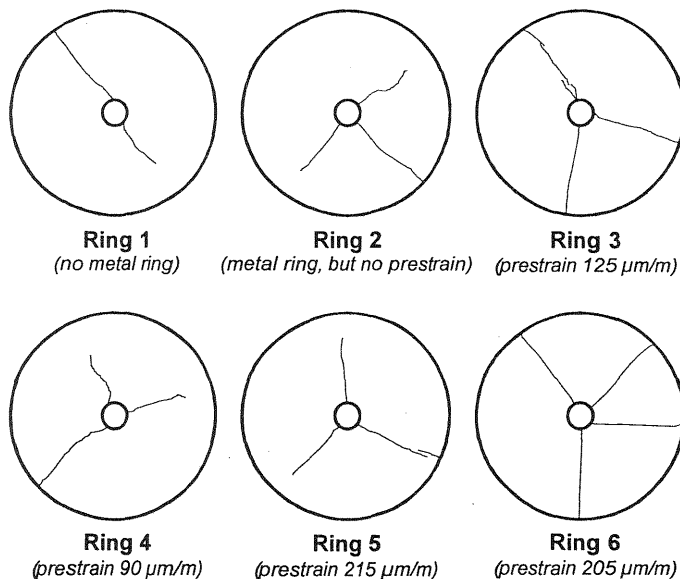

Fig. 3. Crack patterns observed in the experiments
(Numbers in parenthesis refer to the prestrain in the outer metal ring.)

in these specimens (Malvar, 1992; Noghabai, 1995). In addition, a stable crack propagation occurred and the cracks were more uniform in the different directions. In fact, visible cracks formed and propagated without causing the global and unstable failure.
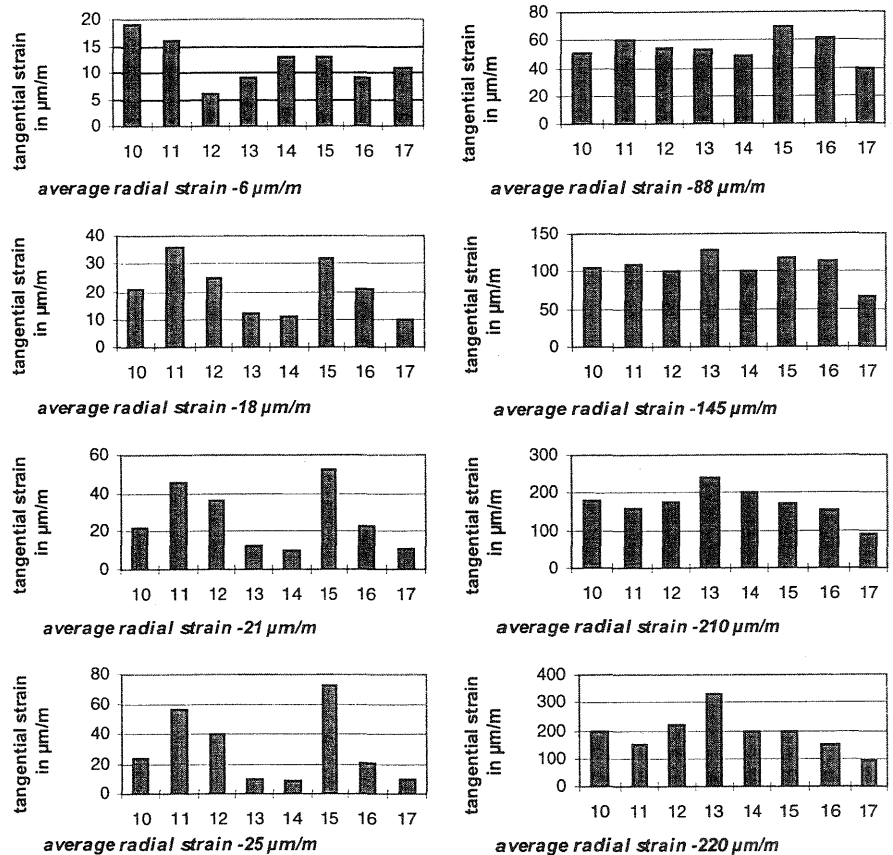

Fig. 4. Tangentitial strain values at different strain gage locations under increasing load

The locations of crack propagation could be identified by increased strains even before the occurrence of visible cracks. However, the higher the prestress in the confining metal ring, the more uniform the distribution of the tangential strain is. This can be seen by comparing tangential strain readings taken at Rings 1 and 6, as shown in Fig. 4. Microcrack formation in a fracture process zone should have occurred where tangential strains were larger than 130 μm/m, which is considered to be the elastic limit strain; this could be confirmed by locally measured residual strains. The local microcracking resulted in a local stress
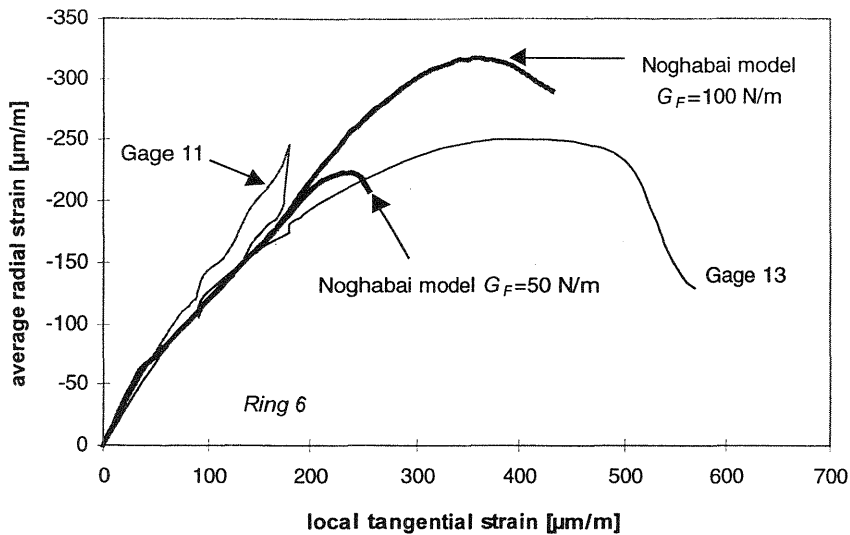
Fig. 5. Local tangential strain versus average radial strain measured from specimen Ring 6

redistribution. Therefore the strain gages next to the one at the crack location showed reduced values due to elastic unloading. Figure 5 shows the local tangential strain in a cracked (Gage 13) and in an uncracked (Gage 11) zone versus the average radial strain, which is considered to be a measure for the load level, as obtained from Ring 6. The different deformation behavior can be noticed.

The theoretical model of Noghabai (1995) was used for a comparison with the experimental results. For doing that, the strains at the gage positions on the specimens (40 mm from the ring inside) were calculated by using this model and the crack opening displacement has been included as an additional smeared tangential strain. Figure 5 also shows the theoretical predictions for a specimen with a chosen number of crack equal to four, as experimentally obtained for specimen Ring 6. Since the theoretical model was developed for a linear softening curve, when the experimentally determined value for the fracture energy (G_F=100 N/m) is used, the measured strains are overestimated by the model because the softening stresses at maximum pressure are too high. In order to simulate the first (steep) branch of the determined bilinear softening by using a linear softening law, a lower fracture energy, equal to 50 N/m, should be used. In this case, the accordance between the experimental observations and the model prediction is better. The initial slope of the linear softening curve used in the model appears to be not steep enough resulting in a too "moderate" stress relief after crack initiation and in an overestimation of the loading capacity and the

1316

maximum strains. This conclusion is confirmed by the comparison of the numerical results with the model predictions.

3 Numerical results

A question which often arose in the papers available in the literature, concerns the number of cracks that form in the concrete ring and influence the global specimen response (Balaguru et al., 1995). The different authors generally considered a uniform pressure distribution in the inner ring. In reality the rib shape of a reinforcing bar is not axisymmetric, as shown in Fig. 6f. Some numerical analyses were here performed to study the effect of the external confinement and of the rib shape on the final crack pattern. The numerical analyses were performed by using MERLIN (Cervenka, Reich and Saouma, 1997) and SBETA (Cervenka Consulting, Prague; Pukl et al., 1992). The first program is based on a discrete crack approach (24 cracks in the concrete ring were allowed), while the latter is based on a smeared crack approach. Contrary to the boundary conditions of the experiments, in the simulation a
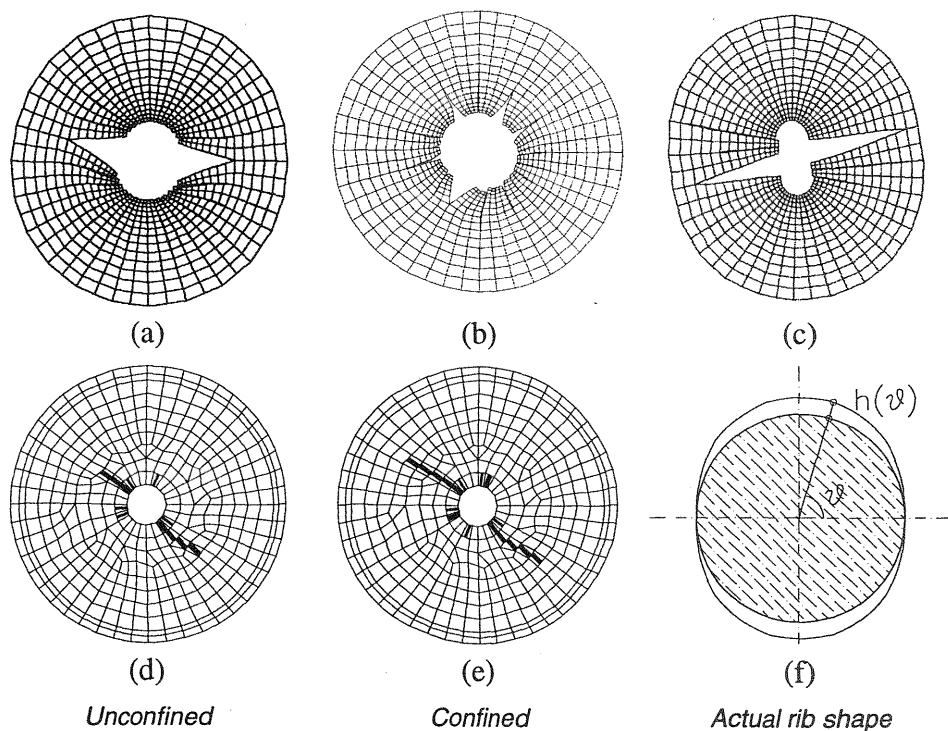

(a)	(b)	(c)
(d)	(e)	(f)
Unconfined	*Confined*	*Actual rib shape*

Fig. 6. Crack patterns obtained in the numerical simulation
(top row: Discrete crack approach; bottom row: Smeared crack approach)

uniform pressure was applied to the inner ring. In addition to the unconfined specimen, the fracture behavior of a specimen with a

confining metal ring subjected to a prestrain of 140 μm/m, which represents an intermediate situation between the specimens Ring 4 and Ring 5, was simulated. These two specimens were both characterised by three cracks at failure.

Figs. 6a,b shows the crack patterns obtained at maximum load from specimens unconfined and confined, respectively, simulated by Merlin. The corresponding crack patterns obtained from SBETA are exhibited in Figs. 6d,e. From both the discrete and the smeared crack approaches, in the unconfined specimens two major cracks could be observed, as in the experiments. In the analyses, initially several cracks form but most of them close, resulting in a final crack pattern characterized by two major cracks splitting the specimen. The same good agreement was obtained for the confined specimens where several cracks are still open at maximum load but three or four of them have a larger crack opening. Figures 7 and 8 show the curves of the inner pressure versus the average radial displacement, as obtained numerically from the confined and unconfined ring, respectively, in comparison with the results from linear elasticity.

The same thick-walled concrete ring under a non-uniform pressure, typical for the rib of an actual rebar, was studied by using the discrete crack approach. The adopted rib shape, schematically shown in Fig. 6f, was measured from an actual 24 mm diameter rebar. The applied inner pressure was proportional to the rib height ($h(\vartheta)$) which varies from zero when $\vartheta=0$, to the maximum value for $\vartheta=90$ degrees (Fig. 6f). The confinement was the same as in the preceeding analysis (3 mm steel ring; prestrain 140 μm/m). As expected, only two cracks formed (Fig. 6c). This result could simplify the analytical models by assuming that only two main splitting cracks form around a rebar with a common rib shape, as experimentally evidenced by Plizzari et al. (1996).

Table 1 contains the maximum pressures obtained from the numerical simulations and by using the model of Noghabai (1995). It can be noticed that the theoretical predictions match the numerical results obtained by using the different FE models very well, especially when the first branch of the softening curve is better approximated (G_F=50 N/m).

Table 1. Maximum pressures applied to the ring specimens (in MPa)

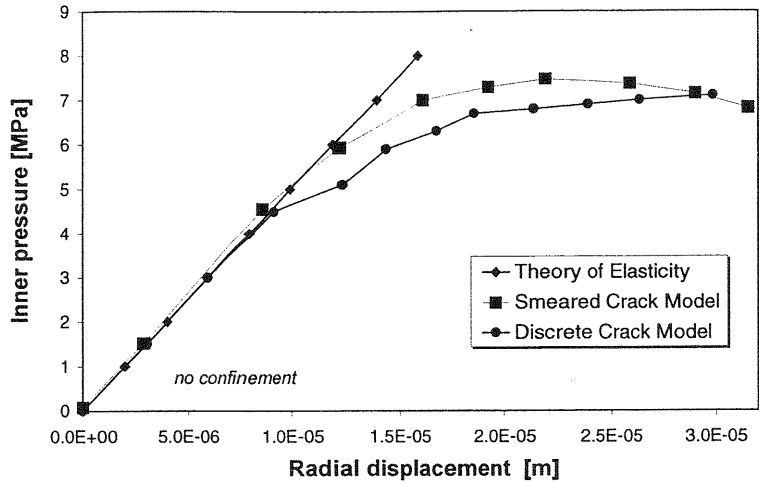| Specimen type	FEM Discrete crack model	FEM Smeared crack model	Model prediction (Noghabai)					
			$G_F = 50$ N/m			$G_F = 100$ N/m		
			n=2	n=3	n=4	n=2	n=3	n=4
Unconfined	7.2	7.4	5.3	7.4	9.1	9.1	11.4	12.7
Confined	9.3	8.6	6.4	9.1	11.2	11.2	14.2	16.1

n ... Number of cracks

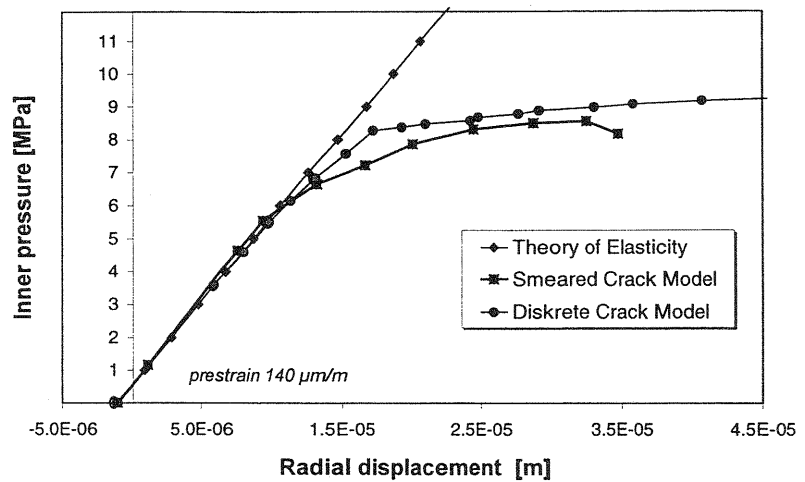Fig. 7. Inner pressure versus radial displacement for the unconfined ring

Fig. 8. Inner pressure versus radial displacement for the confined ring

4 Conclusions

- Experimental results from thick-walled concrete rings were obtained by imposing an outward displacement to the inner surface of the ring to simulate the wedge action of a rebar on the surrounding concrete. Specimens with different external confinements were adopted to simulate the effects of large concrete covers, transverse reinforcement or external pressure.

- A discrete as well as a smeared crack approach were used successfully for simulating the fracture process of the tested specimens.
- The numerical analyses show that in a specimen under a non-uniform inner pressure, typical for an actual shape of a rebar, only two major cracks form. This could simplify some of the bond failure models available in the literature.

Acknowledgements

References

Balaguru, P., Gambarova, P.G., Rosati, G.P. and Schumm C.E. (1995) Bond of reinforcing bars and prestressing tendons in HPFRCC matrices, **Second Int. Workshop on High-Performance Fiber-Reinforced Cement Composites**, eds A. Naaman and H.W. Reinhardt, Ann Arbor (Mi, USA), 325-363.

Cervenka, J., Reich, R.W. and Saouma, V.E. (1997) Merlin, a three dimensional nonlinear finite element program for the fracture mechanics based Investigation of concrete gravity dams and other structures - User's manual, Research Report RP-2917-08, **Electric Power Research Institute**, Palo Alto (CA, USA).

Malvar, L.J. (1992) Bond of reinforcement under controlled confinement, **ACI Materials Journal**, 89(6), 593-601.

Noghabai, K. (1995) Splitting of concrete in the anchoring zone of deformed bars: a fracture-mechanics approach to bond, PhD Thesis, **Div. Struct. Engrg., Luleå University of Technology**, (Sweden).

Plizzari, G.A., Deldossi, A.M. and Massimo, S. (1996) Experimental study on anchored bars in R/C elements with transverse reinforcement, **Materials and Structures**, 29, 534-542.

Pukl, R., Schlottke, B., Ozbolt, J. and Eligehausen, R. (1992) Computer simulation: splitting tests of concrete thick-walled rings, **Proc. 1st Int. Conf. FraMCoS1**, ed. Z.P. Bazant, Elsevier Applied Science, Breckenridge (Co, USA), 367-372.

Reinhardt, H.W. and van der Veen, C. (1990) Splitting failure of a strain-softening material due to bond stresses, **Appl. of Fracture Mech. to Reinf. Concrete**, ed. A. Carpinteri, Elsevier Applied Science, 333-346.

Tepfers, R. (1979) Cracking of concrete cover along anchored deformed reinforcing bars, **Magazine of Concrete Research**, 31(106), 3-12.